Classical and quantum spreading of a charge pulse

B. Gaury, J. Weston, C. Groth, Xavier Waintal

Classical and quantum spreading of a charge pulse

B. Gaury, J. Weston, C. Groth, and X. Waintal
Univ. Grenoble Alpes, INAC-SPSMS, F-38000 Grenoble, France
CEA, INAC-SPSMS, F-38000 Grenoble, France
e-mail: xavier.waintal@cea.fr

***Abstract*—With the technical progress of radio-frequency setups, high frequency quantum transport experiments have moved from theory to the lab. So far the standard theoretical approach used to treat such problems numerically—known as Keldysh or NEGF (Non Equilibrium Green's Functions) formalism—has not been very successful mainly because of a prohibitive computational cost. We propose a reformulation of the non-equilibrium Green's function technique in terms of the electronic wave functions of the system in an energy–time representation. The numerical algorithm we obtain scales now linearly with the simulated time and the volume of the system, and makes simulation of systems with $10^5 - 10^6$ atoms/sites feasible. We illustrate our method with the propagation and spreading of a charge pulse in the quantum Hall regime. We identify a classical and a quantum regime for the spreading, depending on the number of particles contained in the pulse. This numerical experiment is the condensed matter analogue to the spreading of a Gaussian wavepacket discussed in quantum mechanics textbooks.**

I. Introduction

Finite-frequency quantum transport and particle physics are somehow similar; accessing higher frequencies unlocks new physics as the probing frequency crosses characteristic frequencies of the quantum systems. The first of these is the temperature—$\hbar\omega = k_B T$ translates into 20 GHz $\leftrightarrow$ 1 K—and the recent technical progress in assembling radio-frequency lines ($\sim$ 10 GHz) in dilution fridges ($\sim$ 10 mK) have made the domain of time-resolved quantum transport accessible in the lab. This opens the door to the manipulation of very few or even single electrons, a key step towards the development of single electron sources, and in a broader context towards quantum computing. Two different techniques to realize such a source have given promising results. In the first one, an AC signal is applied to a quantum dot which then releases one particle into the connected Fermi sea [1]. This procedure allows a fine control of the energy of the particles, but not of their releasing time. A second route taken in [2] consists of applying a voltage pulse to an Ohmic contact. This technique offers better control of the time-dependence of the source but creates excitations in a wide range of energies. In a single-mode system in the linear regime, such a voltage pulse $V(t)$ induces a current $I(t) = (e^2/h)V(t)$, injecting $\bar{n} = \int eV(t)/h$ particles. These sources have been, up to now, mainly used in the reproduction of known quantum optics experiments [3]. Electrons, however, are not photons and we anticipate many new effects when using the former. In particular, the Fermi sea, always present with fermions but absent in bosonic systems, plays a crucial role.

978-1-4799-5433-9/14/$31.00 © 2014 IEEE

In this manuscript, we first review our wave-function approach (section II) and then focus on a very simple problem: the spreading of a charge pulse in a one-dimensional system (section III). For practical numerical calculations, we simulate the latter using the edge states of a two-dimensional gas in the quantum Hall regime. Therefore the numerics are actually done on a 2D system. In this context, the charge pulses are closely related to the so-called edge magnetoplasmons which have been studied for a long time [4]–[6].

II. From NEGF to a wave function approach

We start with the main results of the Keldysh formalism and completely reformulate it by introducing a time-dependent wave function. We refer to [7]–[9] for more details on the NEGF formalism, and to [10] and references therein for a derivation of the wave function approach and the numerical implementation.

We model an open system with the tight-binding Hamiltonian

$$\hat{\mathbf{H}}(t) = \sum_{i,j} \mathbf{H}_{ij}(t) c_i^\dagger c_j, \tag{1}$$

where $c_i^\dagger$ (c_j) are the Fermionic creation (annihilation) operators of a one-particle state on site i. The system consists of a central region connected to two leads as depicted in Fig. 1. We chose a quasi one-dimensional system for illustrative purposes, but the formalism is completely general and allows the treatment of any multi-terminal device. The basic objects

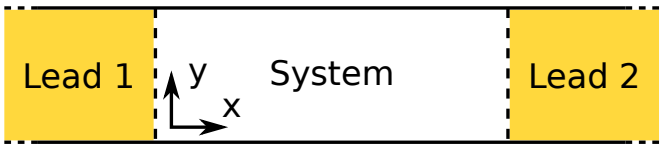

Fig. 1. Schematic of an open system connected to two leads that are kept at equilibrium with temperature $T_{1/2}$ and chemical potential $\mu_{1/2}$.

that we consider are the Retarded (G^R) and Lesser ($G^<$) Green's functions defined in the central region $\bar{0}$. Integrating out the degrees of freedom of the leads, one obtains effective

equations of motion for G^R and $G^<$ [8], [9],

$$i\partial_t G^R(t,t') = \mathbf{H}_{\bar{0}\bar{0}}(t)G^R(t,t') + \int du\ \Sigma^R(t,u)G^R(u,t') \tag{2}$$

$$G^<(t,t') = \int du \int dv\ G^R(t,u)\Sigma^<(u,v)[G^R(t',v)]^\dagger \tag{3}$$

with the initial condition for G^R given by $G^R(t',t') = -i$. The self-energies are spatial boundary conditions that take into account the effect of the leads

$$\Sigma^k(t,t') = \sum_{\bar{m}=1}^{\bar{M}} \Sigma^k_{\bar{m}}(t,t'), \qquad k = R, <, \tag{4}$$

where $\Sigma^k_{\bar{m}}$ is the self-energy of lead $\bar{m}$. The calculation of observables, such as the particle current or the local electronic density, amounts to first solving the integro-differential equation Eq. (2), followed by the double integral of Eq. (3). Physical quantities are then written in terms of the Lesser Green's function. We note N the number of sites inside the system and S the number of sites at the system–lead interfaces. We also note t the maximum time of a simulation and h_t the typical discretization time step. A naive integration of Eq. (2) and Eq. (3) scales as $(t/h_t)^2 S^2 N$. Such a scaling makes the NEGF formalism very demanding from a computational viewpoint. In addition, the integration of Eq. (3) is problematic as the integral converges slowly and large computing times are used simply to recover the equilibrium properties of the system.

The wave function approach allows one to solve these difficulties. One first obtains the stationary wave function $\Psi^{st}_{\alpha E}$ of the system (using for instance the Kwant package developed by some of us[11]) and simply solves the Schrödinger equation,

$$i\partial_t \Psi_{\alpha E}(t) = \mathbf{H}(t)\Psi_{\alpha E}(t) \tag{5}$$

with the initial condition

$$\Psi_{\alpha E}(t<0) = \Psi^{st}_{\alpha E} e^{-iEt} \tag{6}$$

(where we have supposed for convenience that the time-dependent perturbation is only present for $t > 0$). The Lesser Green's function, hence the physical observables (density, current, ...) are then simply expressed in terms of these wave functions,

$$G^<(t,t') = \sum_\alpha \int \frac{dE}{2\pi}\ i f_\alpha(E)\Psi_{\alpha E}(t)\Psi_{\alpha E}(t')^\dagger, \tag{7}$$

where $f_\alpha(E)$ is the Fermi function of lead α. In practice, one considers the deviation to the stationary solution and introduces,

$$\bar{\Psi}_{\alpha E}(t) = \Psi_{\alpha E}(t) - e^{-iEt}\Psi^{st}_{\alpha E}, \tag{8}$$

$\bar{\Psi}_{\alpha E}(t)$ satisfies,

$$i\partial_t \bar{\Psi}_{\alpha E}(t) = W(t)\bar{\Psi}_{\alpha E}(t) + S(t), \tag{9}$$

with $\bar{\Psi}_{\alpha E}(t<0) = 0$ and a "source" term localized where the time-dependent perturbation takes place,

$$S(t) = [\mathbf{H}(t) - \mathbf{H}(t=0)]e^{-iEt}\Psi^{st}_{\alpha E}. \tag{10}$$

Once the wave function starts spreading in the lead, it never comes back, the leads are invariant by translation and therefore full transmitting. The leads are therefore taken into account (exactly) by using absorbing boundary conditions. Eq. (9) can be solved very efficiently in parallel for the different energies and modes.

Fig. 2 illustrates the various approaches taken to describe time-dependent transport. One can consider Green's functions or wave functions, but one can also consider two, apparently different, boundary conditions. In the first [described above by Eq. (5) and (6)] the boundary condition is given for all x and $t = 0$ (this is known in the literature as the partition-free approach). In the second, the scattering approach, one imposes the form of the wave function in the leads (fixed x) at all times t. Both approaches are in fact identical.

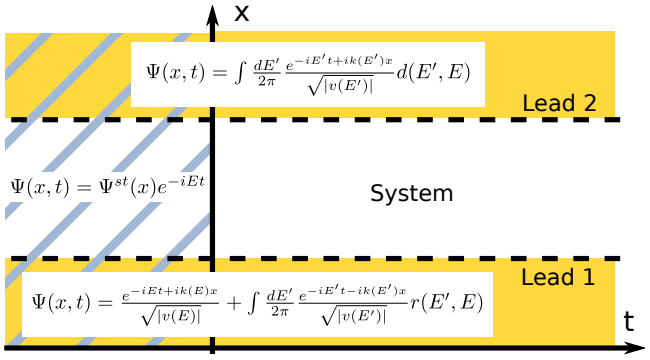

Fig. 2. Boundary conditions for the scattering matrix theory (yellow) and the partition-free approach (blue lines).

III. Spreading of a charge pulse in the quantum Hall regime

We now apply the formalism that has been introduced in the previous section to the spreading of a charge pulse in the quantum Hall regime. We consider a two-dimensional electron gas (2DEG) under high magnetic field connected to two Ohmic contacts as depicted in Fig. 3. We work in a regime where the

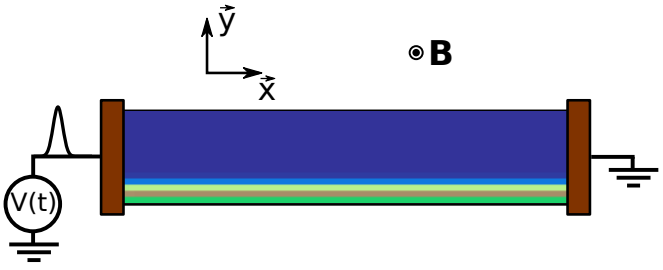

Fig. 3. Color map of $\partial\rho(x,y)/\partial V$ of the two-dimensional electron gas showing the position of the edge state at the Fermi energy.

transport properties are fully determined by the lowest Landau

levels (LLL). We send voltage pulses via the left contact while the right one is grounded. Fig. 3 is not a simple schematic of the system, but shows the electronic charge distribution $\partial\rho(x,y)/\partial V$ appearing in the 2DEG upon applying a DC bias voltage V at the left contact. The Hamiltonian for the system reads

$$\hat{\mathbf{H}} = \frac{(\vec{P} - e\vec{A})^2}{2m^*} + V(\vec{r},t), \tag{11}$$

where $\vec{P} = -i\hbar\vec{\nabla}$, and $\vec{A} = -By\vec{x}$ is the vector potential in the Landau gauge. B is the magnetic field and m^* is the electron effective mass. $V(\vec{r},t)$ contains the voltage pulse applied to the left Ohmic contact and the confining potential due to the mesa boundary. Equation (11) is discretized on a lattice following standard practice [12] with parameters corresponding to a GaAs/AlGaAs heterostructure. We use an electronic density $n_s = 10^{11}$ cm^{-2} which gives a Fermi energy $E_F = 3.47$ meV (or a Fermi wave length $\lambda_F = 79$ nm). We take a magnetic field $B = 1.8$ T that corresponds to a magnetic length $l_B = 19$ nm, and the width of the system is 150 nm.

Fig. 4 shows the propagation of a charge pulse generated by a Lorentzian voltage pulse $V(t) = V_p/(1+(t/\tau_p)^2)$, with amplitude $V_p = 0.5$ mV and duration $\tau_p = 5$ ps, applied to the left contact. We represented the deviation of the electronic charge from equilibrium in the center of mass of the pulse at three different times. The corresponding charge integrated along the y-direction is plotted in Fig. 5a. One observes (i) a ballistic propagation at the Fermi group velocity, (ii) a global spreading of the charge pulse and (iii) oscillations of charge density inside its envelope. A similar feature was already shown in [10] for the propagation of different shapes of voltage pulses (Lorentzian and Gaussian) in a one-dimensional chain. We study the propagation of the pulse in the 2DEG

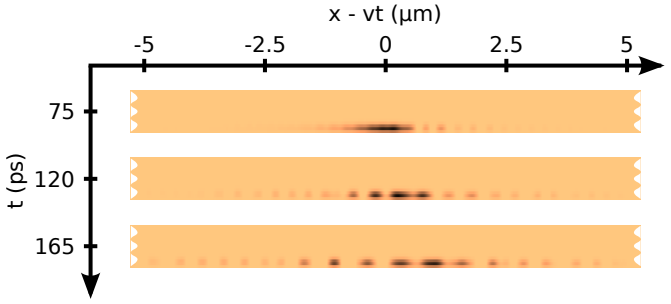

Fig. 4. Charge density color map of the spreading of a charge pulse generated by a Lorentzian voltage pulse, $V(t) = V_p/(1+(t/\tau_p)^2)$, with amplitude $V_p = 0.5mV$ and duration $\tau_p = 5ps$.

within a Landauer-Büttiker approach using the concept of one-dimensional edge states [13]. The system is invariant by translation in the x-direction, hence in absence of voltage pulse the LLL are eigenstates of the Hamiltonian Eq. (11) with the plane waves

$$\psi_k(x,y,t) = e^{-(y-kl_B^2)^2/4l_B^2}\ e^{ikx}. \tag{12}$$

Following the results obtained for a one-dimensional chain [10], we see that in presence of the voltage pulse, ψ_k becomes $\psi = Y\psi_k$. In the case of a Lorentzian pulse an explicit expression can be obtained for the modulation Y in the coordinate of the center of mass of the charge pulse $X = x - vt$,

$$Y(X,t) = 1 - v\tau_P\sqrt{\frac{2m^*\pi}{it}}\exp\left(\frac{m^*(iX - v\tau_P)^2}{2it}\right) \times\left[1 + \mathrm{Erf}\left(\frac{iX - v\tau_P}{2\sqrt{it/(2m^*)}}\right)\right] \tag{13}$$

with $v = \partial E/\partial k$ and the usual definition of the error function $\mathrm{Erf}(x) = (2/\sqrt{\pi})\int_0^x e^{-u^2}du$. It can be shown from Eq. (13) that the oscillations observed in Fig. 4 spread diffusively [10] $\propto \sqrt{t}$ according to the expected behavior of a wave packet in quantum mechanics. However, the width $\Delta X(t)$ of the envelope of the charge density spreads *linearly* in time. $\Delta X(t)$ can be obtained analytically from the exponential decay of $|Y|^2$ with X or numerically by looking at the envelope of the electronic density $\rho(x,y,t)$. In practice, we calculate $Q(x,t) = \int dy \int_0^x d\bar{x}\rho(\bar{x},y,t)$ and define ΔX as the difference between the blue and red crosses in Fig. 5a. We identify two contributions to the spreading as can be seen in Fig. 5b. First we expand the exponential argument in Eq. (13) and find that the spatial extension of the envelope of the charge pulse $\Delta X|_{qu}$ is typically given by

$$\Delta X\Big|_{qu} = \frac{t}{m^*\Delta X_0}, \tag{14}$$

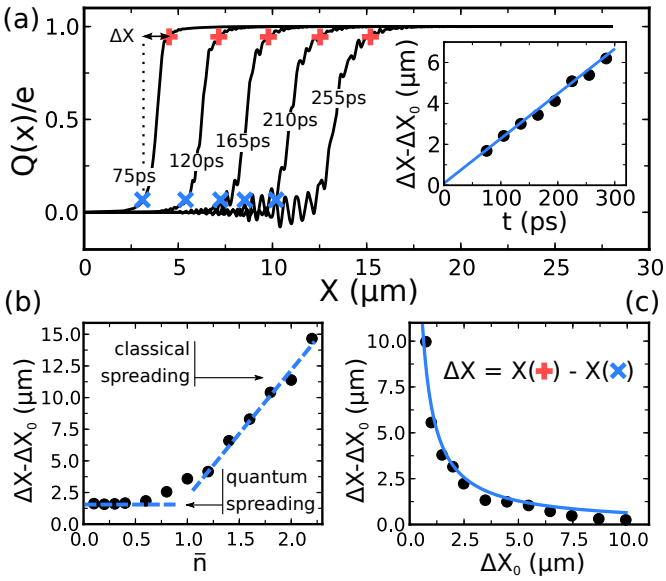

Fig. 5. (a) Number of particles as a function of space (integrated along the y-direction). Symbols correspond to 5% (blue cross) and 95% (red pluses) of the particles sent. Inset: spreading of the charge pulse as a function of time. The full line is a linear fit $\Delta X - \Delta X_0 = at$. (b) Spreading of the charge pulse as a function of the number of particles sent $\bar{n}$. The dots correspond to numerical data and the dashed blue lines guide the eye to distinguish between the quantum and the classical regime. (c) Spreading of the charge pulse as a function of its initial spatial extension. The dots are numerical data and the continuous line correspond to the fit $\Delta X - \Delta X_0 = a/\Delta X_0$. Parameters for the Lorentzian voltage pulse: (a) $\tau_p = 5$ ps, $\bar{n} = 1$, (b) $\tau_p = 5$ ps, (c) $\bar{n} = 1$, with $\bar{n} = (e/h)V_p\tau_p/4$. (b) and (c) are calculated at $t = 200$ ps.

with $\Delta X_0 = v\tau_p$ the initial spatial extension of the pulse. Fig. 5b shows that Eq. (14) is valid only in the quantum regime that is bounded by $\bar{n} \approx 1$. We shall also consider a "hydrodynamic" aspect of the spreading. This second contribution arises when one considers how the various states ψ_k are filled (with Fermi statistics). Upon varying the potential on the left Ohmic contact between 0 and V_p, one injects particles with different energies and hence different velocities into the system. To first order in V_p, we find that the difference of speed between the fastest and the slowest particles is given by $V_p/(vm^*)$. We recast the amplitude of the voltage pulse in terms of the number of particles it contains $\bar{n} \sim V_p\tau_p$. This yields a "classical" component of the spreading of the charge pulse,

$$\Delta X\Big|_{cl} = \frac{\bar{n}t}{m^*\Delta X_0}. \tag{15}$$

The second part of Fig. 5b ($\bar{n} > 1$) confirms the scaling of Eq. (15) with the number of particles injected by the voltage pulse. Overall Fig. 5c confirms the scaling in $1/\Delta X_0$ of Eqs. (14) and (15).

IV. Conclusion

Fast quantum electronics is still an emerging field, both experimentally and, to some extent, theoretically. Our formalism paves the way for the simulation of systems of large size, enabling us to target the physical scales relevant to actual mesoscopic devices. We have shown that the transport properties of a voltage pulse applied to an Ohmic contact are closely related to its quantum nature, that is already expected to exhibit intriguing results [14].

Acknowledgment

This work is funded by the ERC consolidator grant MesoQMC.

References

[1] G. Fève, A. Mahé, J.-M. Berroir, T. Kontos, B. Plaçais, D. C. Glattli, A. Cavanna, B. Etienne, and Y. Jin, "An on-demand coherent single-electron source," *Science*, vol. 316, p. 1169, May 2007.

[2] J. Dubois, T. Jullien, F. Portier, P. Roche, A. Cavanna, Y. Jin, W. Wegscheider, P. Roulleau, and D. C. Glattli, "Minimal-excitation states for electron quantum optics using levitons," *Nature*, vol. 502, pp. 659 – 663, 2013.

[3] E. Bocquillon, V. Freulon, J.-M. Berroir, P. Degiovanni, B. Plaçais, A. Cavanna, Y. Jin, and G. Fève, "Coherence and indistinguishability of single electrons emitted by independent sources," *Science*, vol. 339, no. 6123, pp. 1054–1057, 2013.

[4] I. L. Aleiner and L. I. Glazman, "Novel edge excitations of two-dimensional electron liquid in a magnetic field," *Phys. Rev. Lett.*, vol. 72, pp. 2935–2938, 1994.

[5] N. Kumada, H. Kamata, and T. Fujisawa, "Edge magnetoplasmon transport in gated and ungated quantum hall systems," *Phys. Rev. B*, vol. 84, p. 045314, 2011.

[6] I. Petković, F. I. B. Williams, K. Bennaceur, F. Portier, P. Roche, and D. C. Glattli, "Carrier drift velocity and edge magnetoplasmons in graphene," *Phys. Rev. Lett.*, vol. 110, p. 016801, 2013.

[7] O. Shevtsov and X. Waintal, "Numerical toolkit for electronic quantum transport at finite frequency," *Phys. Rev. B*, vol. 87, p. 085304, Feb 2013.

[8] J. Rammer and H. Smith, "Quantum field-theoretical methods in transport theory of metals," *Rev. Mod. Phys.*, vol. 58, p. 323, Apr 1986.

[9] J. Rammer, *Quantum field theory of non-equilibrium states*. Cambridge Univ. Press, 2007.

[10] B. Gaury, J. Weston, M. Santin, M. Houzet, C. Groth, and X. Waintal, "Numerical simulations of time-resolved quantum electronics," *Physics Reports*, vol. 534, no. 1, pp. 1 – 37, 2014.

[11] C. W. Groth, M. Wimmer, A. R. Akhmerov, and X. Waintal, "Kwant: a software package for quantum transport," *New Journal of Physics*, vol. 16, no. 6, p. 063065, 2014.

[12] K. Kazymyrenko and X. Waintal, "Knitting algorithm for calculating green functions in quantum systems," *Phys. Rev. B*, vol. 77, p. 115119, Mar 2008.

[13] M. Büttiker, "Absence of backscattering in the quantum hall effect in multiprobe conductors," *Phys. Rev. B*, vol. 38, pp. 9375–9389, Nov 1988.

[14] B. Gaury and X. Waintal, "Dynamical control of interference using voltage pulses in the quantum regime," *Nat. Commun.*, vol. 5, p. 3844, 2014.